



1 **Bayesian assessment of chlorofluorocarbon (CFC), hydrochlorofluorocarbon (HCFC) and**
2 **halon banks suggest large reservoirs still present in old equipment**

3
4 Megan Lickley¹, John Daniel², Eric Fleming^{3,4}, Stefan Reimann⁵, Susan Solomon¹

- 5
6 1. Department of Earth, Atmospheric and Planetary Sciences, Massachusetts Institute of
7 Technology, Cambridge, MA 02139, USA
8 2. NOAA Chemical Sciences Laboratory (CSL), Boulder, CO 80305-3328, USA
9 3. NASA Goddard Space Flight Center, Greenbelt, MD, USA
10 4. Science Systems and Applications, Inc., Lanham, MD, USA
11 5. Laboratory for Air Pollution/Environmental Technology, Empa, Swiss Federal
12 Laboratories for Materials Science and Technologies, Duebendorf, Switzerland
13

14 *Correspondence to:* Megan Lickley (mlickley@mit.edu)
15

16 **Abstract**

17 Halocarbons contained in equipment such as air conditioners, fire extinguishers, and foams
18 continue to be emitted after production has ceased. These ‘banks’ within equipment and
19 applications are thus potential sources of future emissions, and must be carefully accounted for
20 in order to evaluate ongoing compliance with the Montreal Protocol. Here, we build on a
21 probabilistic Bayesian model, previously developed to quantify CFC-11, 12 and 113 banks and
22 their emissions. We extend this model to the suite of the major banked chemicals regulated
23 under the Montreal Protocol (HCFC-22, HCFC-141b, and HCFC-142b, halon-1211, and halon-
24 1301, and CFC-114 and CFC-115) along with CFC-11, 12 and 113 in order to quantify a fuller
25 range of ozone-depleting substance banks by chemical and equipment type. We show that if
26 atmospheric lifetime and prior assumptions are accurate, banks are very likely larger than
27 previous international assessments suggest, and that production has been very likely higher than
28 reported. We identify that banks of greatest climate-relevance, as determined by global warming
29 potential weighting, are largely concentrated in CFC-11 foams and CFC-12 and HCFC-22 non-
30 hermetic refrigeration. Halons, CFC-11, and 12 banks dominate the banks weighted by ozone
31 depletion potential. Thus, we identify and quantify the uncertainties in substantial banks whose
32 future emissions will contribute to future global warming and delay ozone hole recovery if left
33 unrecovered.
34

35 **1. Introduction**
36

37 The Montreal Protocol regulates the production of ozone-depleting substances (ODPs), and its
38 implementation has avoided a world with catastrophic ozone depletion (Newman et al., 2009).
39 Globally, there has been a near-cessation of chlorofluorocarbon (CFC) and halon production
40 since 2010, and global production of the replacement hydrochlorofluorocarbons (HCFCs), are
41 scheduled to be phased-out by 2030. Despite production phase-out, these chemicals persist in
42 old equipment produced prior to phase-out, such as refrigeration, air conditioners, foams, and
43 fire extinguishers. These reservoirs of materials (termed ‘banks’) continue to be sources of
44 emissions (e.g., WMO, 2018). Previously published estimates of bank sizes and bank emissions
45 vary widely due to different estimation techniques that incorporate incomplete or imprecise
46 information (TEAP, 2009; WMO, 2003). This uncertainty obscures ongoing emissions
47 attribution and undermines international efforts to evaluate global compliance with the Montreal
48 Protocol. In earlier work, we developed a Bayesian probabilistic banks model for CFCs that



49 incorporates the widest range of constraints to date (Lickley et al., 2020, 2021). Here, we extend
50 this model to the suite of major chemicals regulated by the Protocol that are subject to banking.

51 Previously published assessments typically rely on one of three modeling approaches to
52 estimate bank sizes and to then estimate emissions associated with these banks. In the “top-
53 down” approach (e.g. WMO, 2003), banks are estimated as the cumulative difference between
54 reported production and observationally-derived emissions. However, by taking the cumulative
55 sum of a small difference between two large values, small biases in emissions or production
56 estimates can propagate into large biases in bank estimates (Velders & Daniel, 2014). Some type
57 of bias is thus expected since production has very likely been under-reported to some extent (e.g.
58 Gamlen et al., 1986; Montzka et al., 2018), and emissions estimates rely on observed
59 concentrations along with global lifetime estimates, which have large uncertainties associated
60 with them (SPARC, 2013).

61 The second approach relies on a “bottom-up” accounting method (Ashford et al., 2004;
62 IPCC/TEAP, 2006), where the inventory of sales by equipment type are carefully tallied along
63 with estimated release rates by application use. The bottom-up approach also relies on sales data
64 from surveys of various equipment types and products as well as estimates of their respective
65 leakage rates (SROC, 2005). These are all subject to uncertainties, which contributes to
66 uncertainties in bottom-up bank estimates as well. A limitation of the bottom-up method is that
67 observed atmospheric concentrations are used only as a qualitative check and are not explicitly
68 accounted for in the analysis. Another important limitation is that data used in the bottom-up
69 accounting method are unobserved but rather reported, such as production or sales of equipment,
70 thus bias in reporting could propagate into large biases in bank estimates.

71 The third approach, and the one used in more recent ozone assessments (WMO, 2011, 2014,
72 2018) uses a hybrid approach to calculate banks. Bottom-up banks estimated for 2008 are used
73 as the starting point of the calculations. These banks are taken from SROC (2006) and represent
74 interpolated values from the 2002 and 2015 estimates. The banks are then brought forward to the
75 present time by adding the cumulate reported production and subtracting the cumulative
76 emission from 2008 through the present. This approach is consistent with 2008 bottom-up bank
77 estimates by design, however, as time between 2008 and the present has grown, the cumulative
78 errors associated with the top-down approach have become larger.

79 The modeling approach applied in the present study relies on Bayesian inference of
80 banks (Lickley et al., 2020, 2021) where banks are estimated using an approach called Bayesian
81 parameter estimation. In this approach a simulation model of the bottom-up method is
82 developed, where prior distributions of input parameters are constructed from previously
83 published values, accounting for large uncertainties in production and bank release rates. The
84 simulation model simultaneously models banks, emissions, and atmospheric concentrations.
85 Parameters in the simulation model are then conditioned (or updated) on observed concentrations
86 by applying Bayes’ theory. The final result is a posterior distribution of banks by chemical and
87 equipment type, along with an updated estimate of production and release rates for each
88 equipment type. This approach incorporates data and assumptions from both the bottom-up and
89 top-down approaches, providing a simulation model consistent with the bottom-up accounting
90 approach while also being consistent with observed concentrations within their uncertainties.

91 The remainder of the paper includes the following: Section 2 presents the Bayesian modeling
92 approach along with data used in the analysis. Section 3 provides a summary of the results of
93 our analysis for each of the chemicals considered here. Finally, Section 4 provides a discussion
94 of our primary findings and limitations of the analysis.

95
96

2. Methods



97
98 The Bayesian modeling approach from Lickley et al. (2020, 2021) draws on a Bayesian analysis
99 approach called Bayesian melding, designed by Poole & Raftery (2000), that allows us to apply
100 inference to a deterministic simulation model. We employ a version of this method that we
101 henceforth refer to as Bayesian Parameter Estimation (BPE), which allows for input parameter
102 uncertainty (Bates et al., 2003; Hong et al., 2005). The model flow is implemented as follows;
103 first we develop a deterministic simulation model, representing the “bottom-up” accounting
104 method that simultaneously simulates banks, emissions, and mole fractions for each chemical
105 and equipment type. In this analysis, the chemicals considered include CFC-11, 12, 113, 114,
106 and 115, HCFC-22, 141b, and 142b, and halon-1201, and 1311. Prior distributions for each of
107 the input parameters are based on previously published estimates. We then specify the
108 likelihood function as a function of the difference between observed and simulated mole
109 fractions. Finally, we estimate posterior distributions of both the input and output parameters by
110 implementing Bayes’ Rule using a sampling procedure. Each of the steps of the BPE are
111 described in more detail below.

112 113 **2.1 Simulation Model**

114 The simulation model is comprised of equations (1) – (5) which simultaneously models banks,
115 emissions, and mole fractions for each chemical by equipment type for all years with available
116 data up until 2019. Starting dates differ by chemical, see the Supplement for details. The
117 simulation model is specified as follows;

$$118$$
$$119 B_{j,t+1} = (1 - RF_{j,t}) \times B_{j,t} + (1 - DE_{j,t}) \times P_{j,t} \quad (1)$$
$$120$$

121 where $B_{j,t}$, is banks and $P_{j,t}$ is production of equipment category, j , in year, t . $RF_{j,t}$ reflects the
122 fraction of the bank released and $DE_{j,t}$ reflects the fraction of production that is directly emitted
123 in equipment category, j , year, t . These same parameters are used to simulate emissions, $E_{j,t}$:

$$124$$
$$125 E_{j,t+1} = RF_{j,t} \times B_{j,t} + DE_{j,t} \times P_{j,t} \quad (2)$$
$$126$$

127 Total banks, $B_{Total,t}$, and total emissions, $E_{Total,t}$, are then estimated as the sum across all N
128 equipment categories;

$$129$$
$$130 B_{Total,t} = \sum_{j=1}^N B_{j,t} \quad (3)$$
$$131$$

$$132 E_{Total,t} = \sum_{j=1}^N E_{j,t} \quad (4)$$
$$133$$

134 For chemicals where feedstock usage is reported, an additional term in eq (4) is included that
135 accounts for feedstock emissions. Emissions are then used to simulate atmospheric mole
136 fractions, MF_t , along with an assumed atmospheric lifetime, τ_t , taken as the SPARC (2013)
137 multi-model time-varying mean;

$$138$$
$$139 MF_{t+1} = \exp\left(\frac{-1}{\tau_t}\right) \times MF_t + A \times E_{Total,t} \quad (5)$$
$$140$$

141 where A is a constant that converts units of emissions to units of mole fractions.
142



143

144 2.2 Prior Distributions

145 Prior distributions for each of the input parameters in the simulation model described above are
146 developed to estimate mole fractions, emissions, and banks for CFC-11, 12, 113, 114, and 115,
147 HCFC-22, 141b, and 142b, and halon-1201, and 1311. Categories of bank equipment are
148 defined by the categorization provided by AFEAS (2001), which varies by compound (shown in
149 Table 1). For halons, there is a single category of bank (fire extinguishers).

150 AFEAS data reports global annual production up to 2001 categorized by equipment type,
151 which is generally categorized into short, medium and long-term banks. We use AFEAS data
152 and categorization to develop our production priors and adopt the WMO (2003) correction where
153 AFEAS production values are used up until 1989 and then scaled to match UNEP global
154 production values for all years following 1989. After AFEAS data ends, we assume the relative
155 production in each category remains constant for all years following 2001. Uncertainty in
156 production priors is assumed to follow a multivariate log-normal distribution, where temporal
157 correlation in production reporting bias is estimated in the BPE. Prior distributions differ by
158 chemical and are developed to be wide enough for atmospheric mole fraction priors to contain
159 observations. See the Supplement for details on production priors for each chemical.

160 The emissions function by bank equipment type can be characterized by the fraction of
161 production that is directly emitted during the year of production (DE) and the fraction of the
162 bank that is emitted in each subsequent year. Prior estimates for emissions functions come from
163 previously reported data and differ by chemical and equipment type (see the Supplement).
164 Broadly speaking, it has been estimated that chemicals contained in short-term banks are fully
165 emitted within the first two years after production, medium-term banks lose about 10 – 20% of
166 their material each year, and long-term banks can lose as little as 2% of their material each year
167 (Ashford et al., 2004). We use previously published estimates to develop emissions function
168 priors specific to each chemical and bank type along with wide uncertainties, as specified in the
169 Supplement.

170 Amounts of halocarbons used for feedstock production are available annually
171 (UNEP/TEAP, 2021). A prior mean leakage rate of 2% was assumed during production, which
172 reflects a medium value between different facilities (MCTOC, 2019).

173

174 **Table 1:** Application type of halocarbon banks by chemical

Chemical	Short Bank	Medium Bank	Long Bank
CFC-11	Aerosols Open-cell foam	Non-hermetic refrigeration	Closed-cell foam
CFC-12	Aerosols Open-cell foam	Non-hermetic refrigeration	Refrigeration
CFC-113	solvents		Heat pump
CFC-114			Heat pump
CFC-115	Propellant		Air conditioning
HCFC-22	Open-cell foam	Non-hermetic refrigeration	Foam
HCFC-141b	Open-cell foam	Non-hermetic refrigeration	Foam
HCFC-142b		Non-hermetic refrigeration	Foam
Halon-1211		Fire extinguishers	
Halon-1301		Fire extinguishers	

175

176

177 2.3 Likelihood function



178 For each chemical, the likelihood function is a multivariate normal likelihood function of the
179 difference between modeled and observed mole fractions;

180

$$181 \quad P(D_{t1}, \dots, D_{tN} | \boldsymbol{\theta}) = \frac{1}{(2\pi)^{\frac{N}{2}} \sqrt{|S|}} \exp \left\{ -\frac{1}{2} \Delta^T S^{-1} \Delta \right\} \quad (6)$$

182

183 Where D_{t1}, \dots, D_{tN} is yearly globally-averaged observed mole fractions for all years where
184 observations are available and $\boldsymbol{\theta}$ represents that vector of input and output parameters from the
185 simulation model. Δ is an $N \times 1$ vector of the difference between yearly observed and modeled
186 mole fractions and is assumed to have a mean zero, and covariance function S . S therefore
187 represents the sum of uncertainties between observed and modeled mole fractions. While there
188 are published estimates of uncertainties in observed mole fractions, the uncertainties in modeled
189 mole fractions do not, therefore, we estimate S separately for each chemical, as is done in
190 (Lickley et al., 2020). The off-diagonals in the covariance function incorporate a correlation
191 term, which accounts for our assumption that there is high correlation in the bias between
192 modeled and observed mole fractions. Correlation terms for each chemical are reported in the
193 Supplement along with prior estimates of the uncertainty parameters used for diagonal elements
194 in S . Observations come from the Advanced Global Atmospheric Gas Experiment (AGAGE;
195 <https://agage.mit.edu>) data set (Prinn et al., 2000; Prinn et al., 2018), with the exception of CFC-
196 11 and 12 which, following Lickley et al. (2021), come from the AGAGE and NOAA merged
197 data sets (Engel et al., 2019). Data are aggregated into annual global mean mole fractions. The
198 time frame of availability of observations differs by chemical (see the Supplement).

199

200 **2.4 Posterior Distributions**

201 Following Bayes' Rule, we specify our posterior distribution as;

202

$$203 \quad P(\boldsymbol{\theta} | D_{t1}, \dots, D_{tN}) = \frac{P(\boldsymbol{\theta})P(D_{t1}, \dots, D_{tN} | \boldsymbol{\theta})}{P(D_{t1}, \dots, D_{tN})} \quad (7)$$

204

205 Where $P(\boldsymbol{\theta})$ represents the joint prior distribution of the input and output parameters described
206 in the simulation model in Section 2.1.

207

208 The analytical form of the posterior distribution is intractable. Thus, we estimate the posterior
209 using a sampling procedure (the sampling importance resampling (SIR) method) to estimate the
210 marginal posterior distributions (Bates et al., 2003; Hong et al., 2005; Rubin, 1988). To
211 implement SIR we draw 1,000,000 samples from the priors, run the simulation model, and then
212 resample from the priors 100,000 times using an importance ratio, which is proportional to the
213 likelihood function. These sample sizes were chosen such that multiple iterations of the model
214 produce consistent results.

215

216 **3. Results**

217 Figure 1 shows observed globally averaged mole fractions compared to BPE estimated mole
218 fractions for each chemical. Figure 2 shows BPE estimated and observationally-derived
219 emissions, assuming the SPARC time-varying multi-model mean lifetime for each species.
220 Posterior estimates agree well with observations for the majority of time periods and chemicals.
221 Note, however, that BPE estimates from Lickley et al. (2021) match observed and
222 observationally-derived estimates more closely for CFC-11 than they do in the present analysis.
223 We attribute this difference in consistency to atmospheric lifetimes being assumed in the present



224 analysis, whereas they were inferred in Lickley et al. (2021), which found inferred lifetimes to be
225 somewhat shorter than the SPARC multi-model mean values. Shorter lifetimes would allow
226 modeled mole fractions to decline more quickly following 1990, better matching observations. A
227 notable discrepancy occurs for CFC-115, where modeled mole fractions are increasing
228 throughout the entire simulation period, whereas observed mole fractions from 2000 onwards are
229 relatively constant. This discrepancy could be explained by the large uncertainties in
230 atmospheric lifetimes of CFC-115 (Vollmer et al., 2018), if atmospheric lifetimes are in fact
231 substantially shorter than the SPARC multi-model mean.

232

233 Figure 3 provides a comparison of BPE bank estimates alongside previously published bank
234 estimates. BPE bank estimates are generally higher than other published values. This can be
235 explained by production uncertainties that are accounted for in the present analysis. Our analysis
236 suggests that production has very likely been underreported for nearly all chemicals. Table 2
237 provides a summary of our estimated bias in cumulative reported production throughout the
238 simulation period for each chemical type. With the exception of CFC-113 and CFC-115, we find
239 our inferred cumulative production to be significantly higher than reported production (at the 1-
240 sigma level), with our median estimate suggesting that production was as little as 9% higher than
241 reported for CFC-12 and as high as 50% higher than reported for Halon-1211. We would expect
242 any consistent bias in reported production to be a bias low, since consistent undercounting of
243 production is more plausible than overcounting production. The exception for this would be the
244 base year, which reduction targets are made with reference to. In this instance, we would expect
245 overreporting for this year to be more likely.

246

247 **Table 2:** Estimated bias in cumulative reported production. Values indicate the percent
248 difference between inferred cumulative production from the onset of production to 2019 relative
249 to reported production, for all uses except for feedstock production. Positive values indicate the
250 percent by which inferred production is higher than reported.

Chemical Name	CFC-11	CFC-12	CFC-113	CFC-114	CFC-115
Median inferred bias (16 th , 84 th percentile)	12% (9%, 13%)	9% (7%, 11%)	-1% (-3%, 0%)	11% (9%, 13%)	-1% (-2%, 5%)
Chemical Name	HCFC-22	HCFC-141b	HCFC-142b	Halon-1211	Halon-1301
Median inferred bias (16 th , 84 th percentile)	10% (6%, 13%)	12% (6%, 19%)	22% (17%, 28%)	50% (41%, 59%)	24% (18%, 32%)

251

252

253 Figure 4 shows the breakdown of emissions by equipment type over time. For CFCs, emissions
254 from short-term banks tend to peak around 1990, as spray applications were banned earlier than
255 other applications, after which emissions from medium and long-term banks become more
256 dominant emission sources. This is to be expected as the phase-out of production after 1990
257 would lead to more CFC emissions from existing banks rather than new, short-lived equipment.
258 For HCFC-22, most of the emission throughout the entire time period is from medium banks,
259 which is largely non-hermetic refrigeration. Long banks (i.e. foams) dominate emissions for
260 HCFC-141b, and for HCFC-142b, where both foams and non-hermetic refrigeration are
261 prominent emission sources throughout the simulation period. Estimated feedstock emissions
262 averaged over 2010 – 2019 are shown in Table 3. HCFC-22 is the largest source of feedstock
263 emissions by mass, but CFC-113 feedstock emissions are estimated to be larger when weighted
264 by GWP100 and ODP.

265



266 **Table 3:** Estimated feedstock emissions averaged from 2010 – 2019 from the Bayesian analysis.
267 Emissions are weighted by mass, global warming potential (GWP100) relative to CO₂ over a
268 100-year time horizon, and by ozone depletion potential (ODP)(WMO, 2018).

Feedstock Emissions	CFC-113	HCFC-22	HCFC-142b
By mass	3.4 Gg/yr	9.3 Gg/yr	2.1 Gg/yr
By GWP100	20, 838 Gg/yr	16,591 Gg/yr	4,302Gg/yr
By ODP	2.8 Gg/yr	0.3 Gg/yr	0.1 Gg/yr

269
270 Figure 5 shows the relative quantity of banked materials by chemical type. Banks are weighted
271 by mass (Figure 5a), by global warming potential (GWP100; Figure 5b), and by ozone depleting
272 potential (ODP; Figure 5c). Our best estimate is that the sum of the HCFCs currently comprise
273 about 77% of banks by mass. However, in terms of climate impacts, CFC-11, 12 and HCFC-22
274 are the largest banked materials weighted by GWP100, accounting for 36%, 14%, and 36% of
275 current banks, respectively. When banks are weighted by ODP, CFC-11 and 12 represent 46%
276 and halons also represent 46% of current banked chemicals.
277

278 Figure 6 shows the composition of banks by chemical type. This, together with Figure 5,
279 provides insight into the most prominent banked sources of halocarbons with regards to
280 GWP100 and ODP. In terms of GWP100, CFC-11 banks largely reside in foams, whereas CFC-
281 12 and HCFC-22 are largely in non-hermetic refrigeration; the latter may be more readily
282 recoverable. In terms of ODP, CFC-11 foams and CFC-12 non-hermetic refrigeration remain
283 important, along with halons which are all contained in fire extinguishers, a recoverable
284 reservoir.
285

286

287 **4. Discussion and Conclusions**

288 This analysis suggests that if lifetime assumptions are correct, published bank estimates using
289 either the top-down or bottom-up methods were likely underestimating bank sizes for all banked
290 chemicals due to underreporting of production (see Table 2). The Bayesian approach used in this
291 analysis does not assume production is known, but rather jointly infers production along with the
292 other parameters in the simulation model, providing probabilistic estimates of historical
293 production values. Previously published bank estimates (Ashford et al., 2004; TEAP, 2009;
294 WMO, 2003) do not infer production, but rather assume it is known, or consider different
295 scenarios. We argue that production assumptions have been biased low due to underreporting
296 and thus have led to published bank estimates that were also biased low.
297

298 Discrepancies between observed mole fractions and BPE-derived mole fractions are notable for
299 the suite of chemicals considered here. While the majority fall within the 90% confidence
300 interval throughout most of the time periods, the trends in concentrations between observations
301 and inferred mole fractions do not always agree. This discrepancy could be related to our
302 partitioning of production type following 2003 (i.e. after AFEAS data ends). Another important
303 limitation in this analysis is in the treatment of atmospheric lifetimes, which could also explain
304 some of these discrepancies. The present analysis assumes atmospheric lifetimes are known and
305 equal to the SPARC (2013) time varying multi-model mean lifetimes. However, previous work
306 has indicated potential biases in SPARC lifetimes, for example for CFCs (Lickley et al., 2021).
307 The potential bias in atmospheric lifetimes would result in biased bank estimates in the present
308 manuscript and requires further analysis.
309



310 There are important discrepancies between CFC-113 feedstock emissions inferred here and those
311 estimated in the previous analysis (Lickley et al., 2020). In Lickley et al. (2020), feedstock
312 emissions were assumed to be the difference between observationally-derived emissions and
313 inferred bank emissions. In the present analysis, prior distributions of feedstock production and
314 leakage rates are developed and feedstock emissions are then inferred. In the present analysis,
315 observationally-derived CFC-113 emissions are higher than total BPE inferred emissions at the
316 1-sigma level from 2010 onwards. This suggests that either observationally-derived emissions
317 are too high, or our BPE estimates are too low. In Lickley et al. (2021), we find that atmospheric
318 lifetimes of CFC-113 are very likely lower than the SPARC multi-model time varying mean,
319 used in the present analysis. This would imply that the observationally-derived emissions shown
320 in Figure 2 are biased low, suggesting an even larger discrepancy between BPE inferred total
321 emissions and observationally derived emissions. Therefore, it seems plausible that the
322 discrepancy is due to prior feedstock emissions estimates being biased low due to larger leakage,
323 or CFC-113 is being produced for a use that is not allowed under the Montreal Protocol.

324
325 Finally, some important details about production and destruction were not fully accounted for in
326 this analysis. For one, feedstock priors were only included for CFC-113, HCFC-22, and HCFC-
327 142b, which could be limiting our assessment of the sources of emissions for other chemicals.
328 However, published feedstock values for other chemicals are not available and leakage rates in
329 feedstock applications may be uncertain. Further, we do not consider end-of-life destruction of
330 equipment as there are no published records, to our knowledge, of these processes. Finally, we
331 were not able to account for a more detailed breakdown in production by equipment type than
332 what has been published by AFEAS, which discretizes production into, at most, four categories
333 of equipment, and does not provide data beyond 2003. Without publicly available details of
334 these processes, modeling of banks and emissions will continue to be limited.

335
336 **Code Availability:** All analyses were done in MATLAB. All code used in this work is available
337 at <https://github.com/meglickley/HalocarbonBanks>

338
339 **Data Availability:** The datasets generated and/or analyzed during the current study are available
340 at <https://github.com/meglickley/HalocarbonBanks>

341
342 **Author Contributions.** All authors contributed to the conceptualization of the manuscript.
343 M.L. conducted the analysis. M.L. prepared the manuscript with contributions from all authors.

344
345 **Competing Interests.** The authors declare that they have no conflict of interest.

346
347 **Acknowledgements.** M.L. and S.S. gratefully acknowledge the support of VoLo foundation
348 and grant 2128617 from the atmospheric chemistry division of NSF. AGAGE is supported
349 principally by NASA (USA) grants to MIT and SIO, and also by: BEIS (UK) and NOAA (USA)
350 grants to Bristol University; CSIRO and BoM (Australia); FOEN grants to Empa (Switzerland);
351 NILU (Norway); SNU (Korea); CMA (China); NIES (Japan); and Urbino University (Italy).

352
353
354 **References**

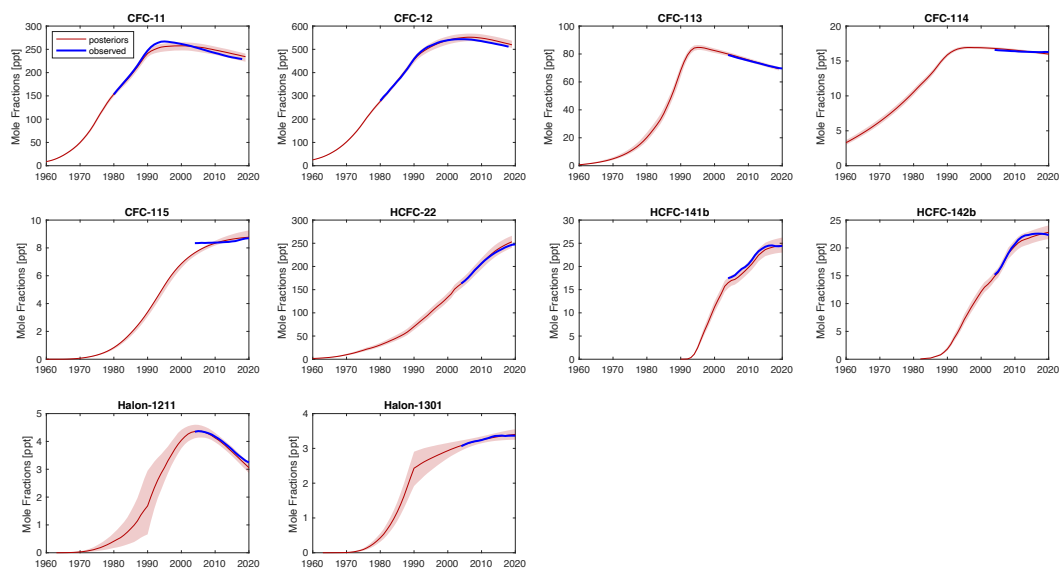
355 AFEAS. (2001). AFEAS 2001 database. Retrieved from
356 [https://unfccc.int/files/methods/other_methodological_issues/interactions_with_ozone_layer](https://unfccc.int/files/methods/other_methodological_issues/interactions_with_ozone_layer/application/pdf/cfc1100.pdf)
357 [/application/pdf/cfc1100.pdf](https://unfccc.int/files/methods/other_methodological_issues/interactions_with_ozone_layer/application/pdf/cfc1100.pdf)



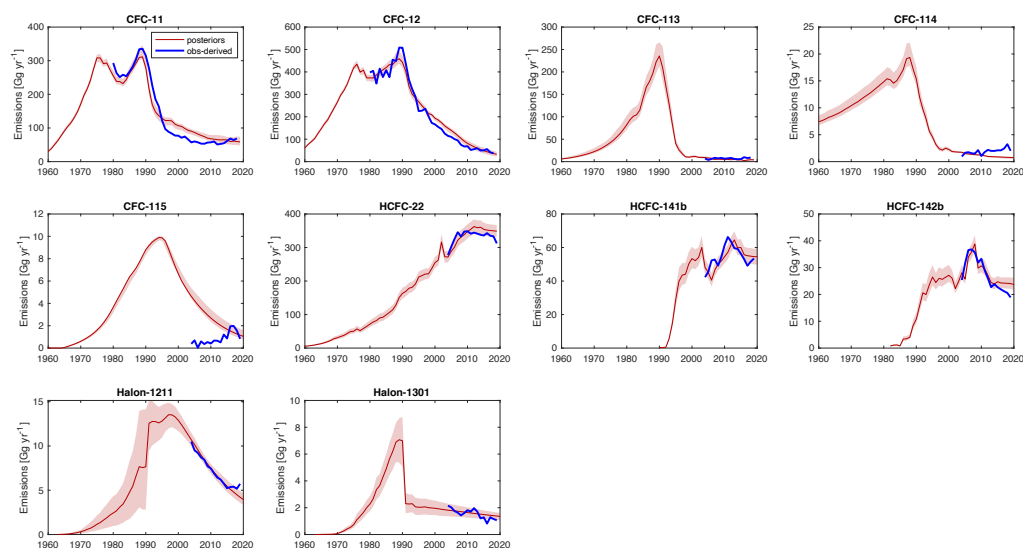
- 358 Andersen, S. O., Metz, B., Kuijpers, L., & Solomon, S. (Eds.). (2005). *Safeguarding the Ozone*
359 *Layer and the Global Climate System: Special Report of the Intergovernmental Panel on*
360 *Climate Change*. Cambridge University Press.
- 361 Ashford, P., Clodic, D., McCulloch, A., & Kuijpers, L. (2004). Emission profiles from the foam
362 and refrigeration sectors comparison with atmospheric concentrations. Part 1: Methodology
363 and data. *International Journal of Refrigeration*, 27(7), 687–700.
- 364 Bates, S. C., Cullen, A., & Raftery, A. E. (2003). Bayesian uncertainty assessment in
365 multicompartment deterministic simulation models for environmental risk assessment.
366 *Environmetrics: The Official Journal of the International Environmetrics Society*, 14(4),
367 355–371.
- 368 Engel, A., Rigby, M., Burkholder, J. B., Fernandez, R. P., Froidevaux, L., Hall, B. D., et al.
369 (2019). *Update on Ozone-Depleting Substances (ODSs) and other gases of interest to the*
370 *Montreal Protocol, Chapter 1 in Scientific Assessment of Ozone Depletion: 2018, Global*
371 *Ozone Research and Monitoring Project - Report No. 58*. Geneva, Switzerland: World
372 Meteorological Organization.
- 373 Gamlen, P. H., Lane, B. C., Midgley, P. M., & Steed, J. M. (1986). The production and release to
374 the atmosphere of CCl₃F and CCl₂F₂ (chlorofluorocarbons CFC11 and CFC 12).
375 *Atmospheric Environment*, 20(6), 1077–1085.
- 376 Hong, B., Strawderman, R. L., Swaney, D. P., & Weinstein, D. A. (2005). Bayesian estimation
377 of input parameters of a nitrogen cycle model applied to a forested reference watershed,
378 Hubbard Brook Watershed Six. *Water Resources Research*, 41(3).
- 379 IPCC/TEAP. (2006). *Task Force on Emissions Discrepancies Report, Technical Report*. Nairobi,
380 Kenya.
- 381 Lickley, M., Solomon, S., Fletcher, S., Rigby, M., Velders, G. J. M., Daniel, J., et al. (2020).
382 Quantifying contributions of chlorofluorocarbon banks to emissions and impacts on the
383 ozone layer and climate. *Nature Communications*, 11(1380).
384 <https://doi.org/10.1038/s41467-020-15162-7>
- 385 Lickley, M., Fletcher, S., Rigby, M., & Solomon, S. (2021). Joint Inference of CFC lifetimes and
386 banks suggests previously unidentified emissions. *Nature Communications*, 12(2920), 1–10.
387 <https://doi.org/https://doi.org/10.1038/s41467-021-23229-2> |
- 388 MCTOC. (2019). *Medical and Chemical Technical Options Committee, 2018 assessment*.
389 Retrieved from [https://ozone.unep.org/sites/default/files/2019-04/MCTOC-Assessment-](https://ozone.unep.org/sites/default/files/2019-04/MCTOC-Assessment-Report-2018.pdf)
390 [Report-2018.pdf](https://ozone.unep.org/sites/default/files/2019-04/MCTOC-Assessment-Report-2018.pdf)
- 391 Montzka, S. A., Dutton, G. S., Yu, P., Ray, E., Portmann, R. W., Daniel, J. S., et al. (2018). An
392 unexpected and persistent increase in global emissions of ozone-depleting CFC-11. *Nature*,
393 557(7705), 413.
- 394 Newman, P. A., Oman, L. D., Douglass, A. R., Fleming, E. L., Frith, S. M., Hurwitz, M. M., &
395 Kawa, S. R. (2009). What would have happened to the ozone layer if chlorofluorocarbons
396 (CFCs) had not been regulated? *Atmospheric Chemistry and Physics*, 9(6), 2113–2128.
- 397 Poole, D., & Raftery, A. E. (2000). Inference for deterministic simulation models: the Bayesian
398 melding approach. *Journal of the American Statistical Association*, 95(452), 1244–1255.
- 399 Prinn, R. G., Weiss, R. F., Fraser, P. J., Simmonds, P. G., Cunnold, D. M., Alyea, F. N., et al.
400 (2000). A history of chemically and radiatively important gases in air deduced from
401 ALE/GAGE/AGAGE. *Journal of Geophysical Research Atmospheres*, 105(D14), 17751–
402 17792. <https://doi.org/10.1029/2000JD900141>
- 403 Prinn, Ronald G., Weiss, R. F., Arduini, J., Arnold, T., Langley Dewitt, H., Fraser, P. J., et al.
404 (2018). History of chemically and radiatively important atmospheric gases from the
405 Advanced Global Atmospheric Gases Experiment (AGAGE). *Earth System Science Data*,



- 406 10(2), 985–1018. <https://doi.org/10.5194/essd-10-985-2018>
- 407 Rubin, D. B. (1988). Using the SIR algorithm to simulate posterior distributions (with
408 discussion). *Bayesian Statistics*, 3, 395–402.
- 409 SPARC. (2013). SPARC Report on the Lifetimes of Stratospheric Ozone-Depleting Substances,
410 Their Replacements, and Related Specied. (M. Ko, P. Newman, S. Reimann, & Strahan S.,
411 Eds.). SPARC Report N. 6, WCRP-15/2013.
- 412 TEAP. (2009). *TEAP (Technology and Economic Assessment Panel), Task Force Decision XX/8*
413 *Report, Assessment of Alternatives to HCFCs and HFCs and Update of the TEAP 2005*
414 *Supplement Report Data*. Nairobi, Kenya. Retrieved from
415 [http://ozone.unep.org/teap/Reports/TEAP_%0AReports/teap-may-2009-decisionXX-8-task-](http://ozone.unep.org/teap/Reports/TEAP_%0AReports/teap-may-2009-decisionXX-8-task-forcereport.%0Apdf)
416 [forcereport.%0Apdf](http://ozone.unep.org/teap/Reports/TEAP_%0AReports/teap-may-2009-decisionXX-8-task-forcereport.%0Apdf)
- 417 UNEP/TEAP. (2021). *TEAP Progress Report Volume I*. Nairobi, Kenya. Retrieved from
418 <https://ozone.unep.org/system/files/documents/TEAP-2021-Progress-report.pdf>
- 419 Velders, G. J. M., & Daniel, J. S. (2014). Uncertainty analysis of projections of ozone depleting
420 substances: mixing ratios, EESC, ODPs, and GWPs. *Atmospheric Chemistry and Physics*,
421 14(6), 2757–2776.
- 422 Vollmer, M. K., Young, D., Trudinger, C. M., Mühle, J., Henne, S., Rigby, M., et al. (2018).
423 Atmospheric histories and emissions of chlorofluorocarbons CFC-13
424 (CClF₃), ΣCFC-114
425 (C₂ClF₂ and C₂F₄), and . *Atmospheric Chemistry and*
426 *Physics*, 18(2), 979–1002. <https://doi.org/10.5194/acp-18-979-2018>
- 427 WMO. (2003). WMO: Scientific Assessment of Ozone Depletion: 2002, Global Ozone Research
428 and Monitoring Project – Report No. 47. Geneva, Switzerland: World Meteorological
429 Organization (WMO),.
- 430 WMO. (2011). *Scientific Assessment of Ozone Depletion: 2010, Global Ozone Research and*
431 *Monitoring Project-Report No. 52*. Geneva, Switzerland.
- 432 WMO. (2014). *Scientific Assessment of Ozone Depletion: 2014, World Meteorological*
433 *Organization, Global Ozone Research and Monitoring Project-Report No. 55*. Geneva,
434 Switzerland.
- 435 WMO. (2018). WMO: Scientific Assessment of Ozone Depletion: 2018, Global Ozone Research
436 and Monitoring Project – Report No. 58. Geneva, Switzerland: World Meteorological
437 Organization (WMO),.
- 438
439
440
441



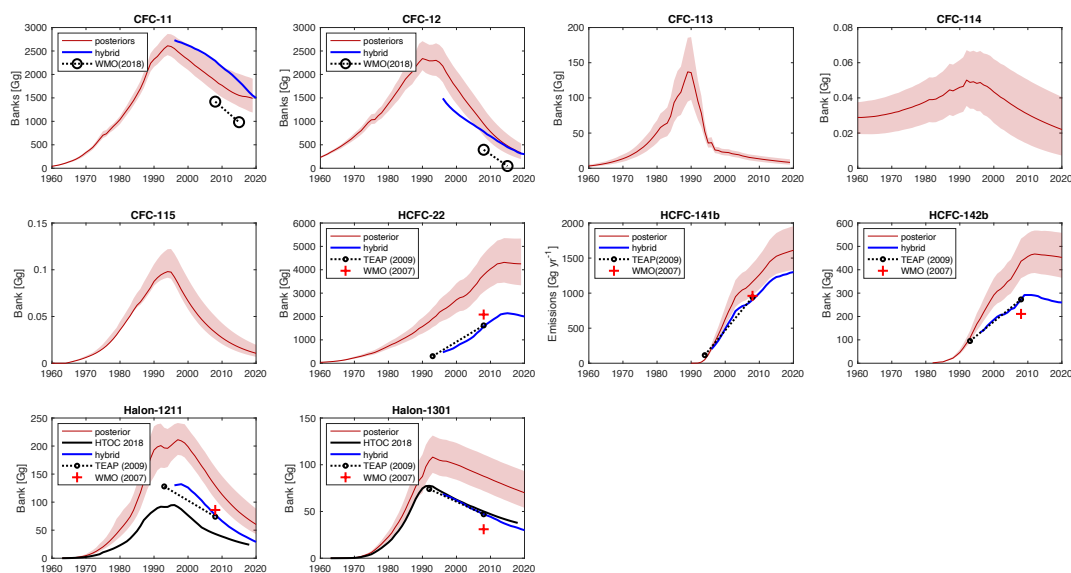
442
443 **Figure 1:** Modeled mole fractions versus observed mole fractions. Red lines indicate the
444 posterior median mole fraction estimate from the Bayesian analysis (BPE), with shaded regions
445 indicating the 90% confidence interval. Blue line indicates globally-averaged observed mole
446 fractions.
447



448
449 **Figure 2:** Modeled emissions versus observationally-derived emissions. Red lines indicate the
450 posterior median emissions estimate from the Bayesian analysis (BPE), with shaded regions
451 indicating the 90% confidence interval. Blue line indicates observationally-derived emissions
452 assuming the SPARC multi-model mean time-varying lifetimes.
453

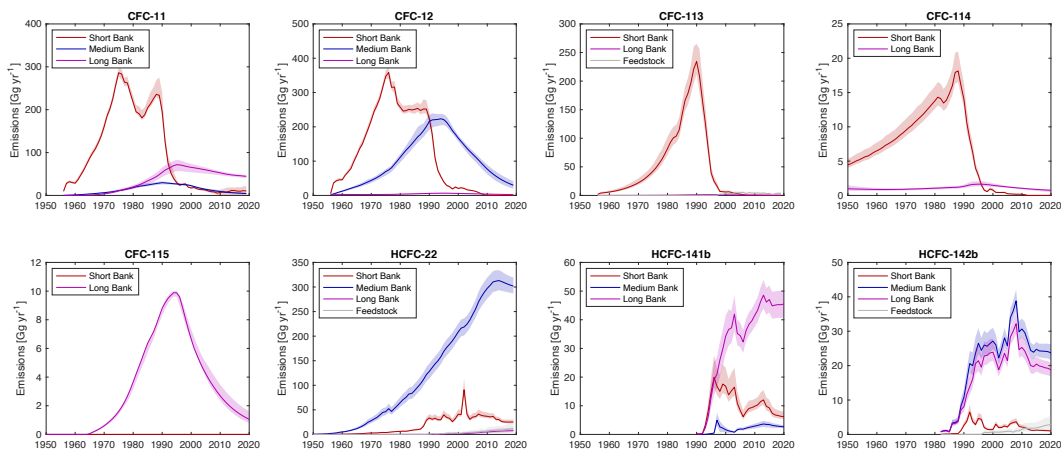


454



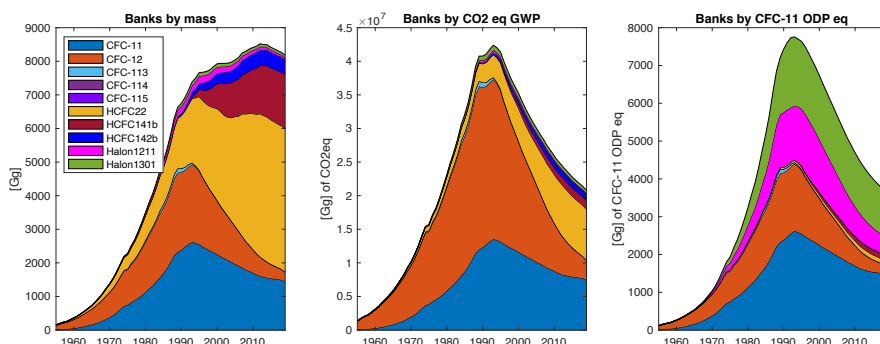
455
 456
 457
 458
 459
 460
 461

Figure 3: Magnitudes of Bank estimates. The red line indicates the median posterior estimate of Banks from the Bayesian analysis, with shading indicating the 90% confidence interval. Previously published bank estimates are provided for comparison from TEAP (2009), WMO (2007), and WMO (2018), along with the hybrid approach updated to current estimated starting values.

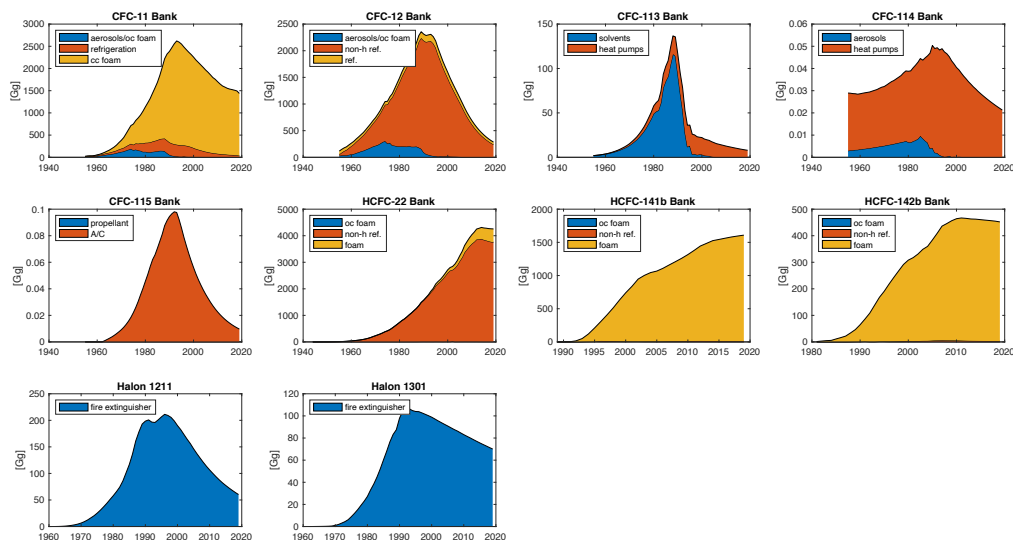


462
 463
 464
 465
 466
 467

Figure 4: Emissions by Source. Emissions estimates by various equipment types, summarized in Table 1, are shown here along with estimated emissions from feedstock usage. Lines indicate the median estimate, with the shaded region indicating the 90% confidence interval. Halons are not included in this figure as 100% of halon emissions come from the same application and are thus identical to Figure 2 halon totals.



468
 469 **Figure 5:** Total banks by mass, global warming potential (GWP100; WMO, 2018) and ozone
 470 depleting potential (ODP; WMO, 2018). Bank estimates reported in the above figures are the
 471 median estimates from the Bayesian analysis.
 472



473
 474 **Figure 6:** Bank size by equipment type. Bank estimates reported in the above figures are the
 475 median estimates from the Bayesian analysis. In the above legends, cc refers to closed-cell
 476 foams, non-h ref. refers to non-hermetic refrigeration, ref. refers to refrigeration, and A/C refers
 477 to air conditioning.
 478